Progress In Electromagnetics Research Letters, Vol. 12, 79–85, 2009

EXPERIMENT AND SIMULATION ON TE_{10} CUT-OFF REFLECTION PHASE IN GENTLE RECTANGULAR DOWNTAPERS

H. Soekmadji, S. L. Liao, and R. J. Vernon

Electrical and Computer Engineering
University of Wisconsin
1415 Engineering Drive, Madison, Wisconsin 53706, USA

Abstract—The phase of the reflection coefficient of a TE_{10} rectangular waveguide mode at the cut-off point in a gentle downtaper is investigated through both experiment and computer simulation. The result shows a very good agreement with the theoretical prediction based on the work by Katsenelenbaum et al., that is, a $+90°$ phase shift occurs at the cut-off point for TE modes if the cut-off point is not too close to the end of the downtaper. An application for the determination of the resonant frequencies for the spurious trapped TE_{30} mode in an uptaper-downtaper oversized resonant structure is presented.

1. INTRODUCTION

The waveguide uptaper-downtaper is important in traditional gyrotrons and gyroklystron resonant cavities [1, 2] as well as in the tapered gyro-Backward-Wave Oscillators (gyro-BWO) for mode confinement [3]. The waveguide uptaper-downtaper is also used in mode converter systems to confine unwanted spurious modes because of the reflection at the cut-off points, causing deep and narrow resonances [4]. Moreover, the downtapered probe has been used in the Near-field Scanning Optical Microscopy (NSOM) [5] and even in the microwave near-field microscopy [6].

The reflection of the electromagnetic wave propagation in the E-plane-tapered and pyramidally-tapered waveguides far above the cut-off frequency have been studied by Matsumaru [7] and Johnson [8]. The electromagnetic fields in the cut-off regime was also theoretically studied by Knoll et al. [6, 9] in the tapered rectangular probe for NSOM application. Furthermore, theoretical work had been done by

Corresponding author: S. L. Liao (shaolin.liao@gmail.com).

Katsenelenbaum et al. [10] on the phase behavior of the TE and TM modes at the cut-off point, in a cross-section approach, where they predicted that the phase of the reflection coefficient at the cut-off point is +90° for TE modes if the downtaper is sufficiently gentle, provided that the cut-off point is not too close to the end of the downtaper. However, a number of approximations have been made in their derivation [10] and it is difficult to quantify them. The reflection coefficient at the cut-off cross section is important in the study of spurious trapped modes in both rectangular and circular waveguide geometries and an experimental verification of the theoretical result appears not to have been undertaken previously.

2. BACKGROUND THEORY

In this research, we mainly focus on the experiment and computer simulation of the H-plane linear rectangular downtaper, in which only the dominant TE_{10} mode was incident, at the frequency regime of 5 GHz–7 GHz. We expect that, although different in frequency and geometry (e.g., cylindrical shape instead of rectangular shape), similar behaviors will appear in the downtapered structures used in gyrotrons, gyroklystrons, gyro-BWOs and in the tapered probe for the NSOM application. Generally, in a downtapered waveguide, the coupling between the incident and reflected waves has to be taken into account, even before it reaches the immediate vicinity of the cut-off point. However, for a gentle downtapered waveguide like the one we used in our experiment, Katsenelenbaum et al. [10] and Xu et al. [11] have shown that this coupling is weak, except in the region close to the cut-off point; hence the mode conversion to the reflected wave may often be neglected except in the region close to the cut-off point.

Let us begin by considering the wave solution of a linear rectangular downtaper (cf. Fig. 1), with a single waveguide mode (TE_{m0} in this case) incident on the larger (input) port. The scalar Helmholtz equation of the TE_{m0} mode for the linear rectangular downtaper is

$$F''(z) + \beta_m^2(z)F(z) = 0, \tag{1}$$

where $\beta_m(z) = \sqrt{k^2 - [m\pi/a(z)]^2}$, with k being the wave number in free space. The WKB solution of (1) may be used if the condition on the waveguide mode phase factor β_m,

$$\left|\frac{\partial \beta_m(z)}{\partial z}\right| \ll \left|\beta_m^2(z)\right|, \tag{2}$$

is satisfied, i.e., the structure is slowly downtapered. The inequality (2) is known to be the region where the geometrical optics approximation is valid [10, 11]. With a time dependence $\exp^{j\omega t}$ being assumed, the solution to (1) is approximately given as the combination of the forward and backward waves,

$$F \sim C_1 \frac{\exp(-j\Phi)}{\sqrt{\beta_m(z)}} + C_2 \frac{\exp(+j\Phi)}{\sqrt{\beta_m(z)}}, \tag{3}$$

where $\Phi = \int \beta_m(z)\ dz + \Phi_0$, with Φ_0 being the constant term determined from the reference point of integration.

Now consider a waveguide mode being applied at the larger (input) port of a rectangular downtaper of length L_{taper} and with broadwall dimension $a(z)$, where $\hat{z}$ is the direction of wave propagation (cf. Fig. 1). The phase delay that is acquired by the incident mode from the input port at $z = 0$, to the cut-off point at $z = z_c$, with $a(z_c) = \lambda/2$, can be found to be

$$\Phi_{\text{taper}} = -\int_0^{z_c} \beta_m(z)\ dz \qquad\qquad 0 \leq z_c < L_{\text{taper}}. \tag{4}$$

The phase of the reflection coefficient Φ_Γ evaluated at the lager (input) port can then be written as

$$\Phi_\Gamma = 2\ \Phi_{\text{taper}} + \Phi_{\text{c}}, \tag{5}$$

where Φ_{c} is the phase of the reflection coefficient at the cut-off point (sufficiently far from the output port).

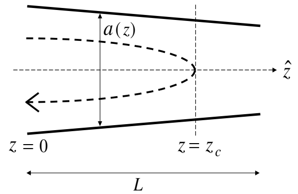

Figure 1. The reflection at the cut-off point in a gentle rectangular downtaper. L is measured parallel to the direction of wave propagation in $\hat{z}$ direction. $a(z)$ is the broadwall dimension of the rectangular downtaper. z_c is the cut-off point where the incident mode is totally reflected back towards the input port.

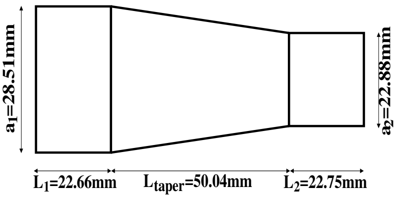

Figure 2. The commercial WR112-WR90 waveguide downtaper. The broadwall dimensions are $a_1 = 28.51$ mm and $a_2 = 22.88$ mm. The longitudinal dimensions are $L_1 = 22.66$ mm, $L_2 = 22.75$ mm, and $L_{\text{taper}} = 50.04$ mm for the downtaper. The cut-off frequency for the TE_{10} mode at Port 1 (larger port) is $f_{c1} = 5.26$ GHz and at Port 2 (smaller port) is $f_{c2} = 6.55$ GHz.

3. MEASUREMENT AND SIMULATION RESULTS

To experimentally verify (5), we considered a commercially available rectangular downtaper shown in Fig. 2. This is a linear downtaper with a rectangular cross section. We shall restrict our investigation to the case where only the TE_{10} mode can propagate from the input port (Port 1 in Fig. 2). For the purpose of analysis, we take the input port to have the larger cross section. The output port (Port 2 in Fig. 2) may be terminated by a matched or short load and is usually far enough from the cut-off point in the downtaper for our research.

In the computer simulation, Cascade (Calabazas Creek Research) and HFSS (Ansoft) were used to obtain Φ_Γ at the larger (input) port. Cascade is a mode-matching software developed by Calabazas Creek Research and HFSS is a finite-element-method software from Ansoft. In Cascade, we simulated the full structure of the downtaper; while in HFSS, simulations for the downtaper were carried out for both the full structure geometry and 1/4 of the full structure (by slicing the downtaper according to the E- and H-planes of symmetries). They both yielded identical results.

We considered cases of both the matched load and shorted load in our experiment. From Fig. 2 and using (5), the phase of the reflection coefficient at the cut-off point is

$$\Phi_{\mathrm{c}} = \Phi_\Gamma + 2\left(\beta_1 L_1 - \Phi_{\mathrm{taper}}\right), \tag{6}$$

where β_1 is the phase constant of TE_{10} mode at $\hat{z}$ direction, in the input uniform rectangular waveguide with length L_1 (cf. Fig. 2). The results from (6) are tabulated in Table 1 and Table 2, where Φ_Γ is the measured quantity in the experiment.

It can be seen from both Table 1 and Table 2 that the calculated Φ_{c} is $+90^\circ$ (within the experimental standard deviation) when z_c is sufficiently far away from the output port such that the wave has decayed significantly by the time it reaches the output port. However, also note that Φ_{c} is no longer close to $+90^\circ$ as z_c approaches the output port, which implies that the structure beyond z_c (matched or short load) affects the phase of the reflection coefficient Φ_Γ at the input port when z_c is close to the output port, as expected [10, 11]. We thus conclude that the theoretical value of Φ_{c} to be $+90^\circ$ for the TE modes is valid for this structure. This allows us to use $\Phi_{\mathrm{c}} = +90^\circ$ for the phase of the reflection coefficient at the cut-off point for gentle rectangular downtapers with a reasonably good approximation.

Table 1. Φ_Γ and Φ_c in WR112-WR90 rectangular downtaper with a matched load.

Freq. (GHz)	L_1+z_c (mm)	Experiment $\Phi_\Gamma(°)$	Experiment $\Phi_c(°)$	HFSS $\Phi_\Gamma(°)$	HFSS $\Phi_c(°)$	Cascade $\Phi_\Gamma(°)$	Cascade $\Phi_c(°)$
5.51	34.26	−30.00	90.74	——	——	−25.73	95.01
5.55	36.00	−46.88	88.43	——	——	−43.66	91.65
5.60	38.15	−65.00	88.61	−63.75	89.86	−64.34	89.27
5.65	40.25	−85.00	87.09	——	——	−84.76	87.32
5.70	42.32	−102.50	88.27	−103.13	87.64	−104.66	86.10
5.75	44.35	−122.50	87.19	——	——	−123.76	85.92
5.80	46.35	−140.63	88.22	−142.50	86.35	−143.15	85.70
5.85	48.32	−160.00	88.27	——	——	−162.48	85.78
5.90	50.25	−180.00	87.95	180.00	87.94	178.58	86.52
5.95	52.14	168.75	96.63	——	——	159.03	86.90
5.99	53.64	153.75	97.75	——	——	143.47	87.47

Table 2. Φ_Γ and Φ_c in WR112-WR90 rectangular downtaper with a short load.

Freq. (GHz)	L_1+z_c (mm)	Experiment $\Phi_\Gamma(°)$	Experiment $\Phi_c(°)$	HFSS $\Phi_\Gamma(°)$	HFSS $\Phi_c(°)$	Cascade $\Phi_\Gamma(°)$	Cascade $\Phi_c(°)$
5.98	53.27	150.00	89.96	150.00	89.95	147.42	87.37
6.00	54.01	142.50	90.56	142.50	90.55	139.20	87.25
6.05	55.84	123.75	92.24	123.75	92.23	119.41	87.89
6.10	57.65	102.50	91.67	103.13	92.28	98.63	87.79
6.15	59.42	82.50	92.58	82.50	92.57	77.83	87.90
6.20	61.17	61.88	93.11	62.50	93.71	55.79	87.00
6.25	62.89	41.25	93.85	41.25	93.84	34.11	86.70
6.30	64.58	20.00	94.19	20.00	94.18	9.63	83.81
6.35	66.25	−5.63	90.37	−1.88	94.11	−14.20	81.79
6.40	67.89	−22.50	95.52	−24.38	93.63	−40.96	77.05
6.45	69.50	−45.00	95.25	−46.88	93.36	−69.42	70.81
6.50	71.09	−67.50	95.17	−67.50	95.15	−103.15	59.50

4. APPLICATION IN MICROWAVE CAVITIES

The phase of the reflection coefficient at the cut-off point Φ_c can be used to determine the resonant frequency of the spurious trapped

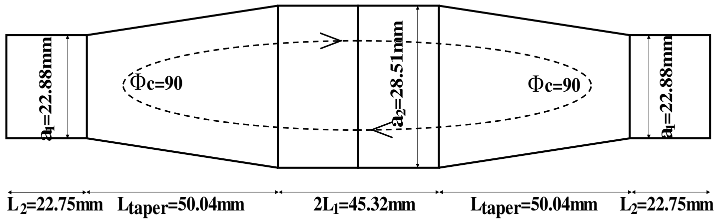

Figure 3. A downtaper-uptaper structure for spurious TE_{30} resonant frequency determination. The structure contains two identical downtapers shown in Fig. 2.

Table 3. Resonant frequencies from (7) and Cascade simulation.

n	f_n (GHz) from (7)	f_n (GHz) from Cascade	Δf_n (GHz)
0	15.85	15.91	−0.06
1	16.28	16.27	0.01
2	16.77	16.76	0.01
3	17.25	17.27	−0.02
4	17.72	17.73	−0.01

modes. Fig. 3 shows the trapped TE_{30} mode in an oversized resonant structure, from which the resonant frequency can be estimated as

$$4\left(\beta_3 L_1 - \Phi_{\text{taper}}\right) - \pi = 2n\pi, \qquad n = 0, 1, 2, \ldots, \tag{7}$$

where β_3 is the phase constant of TE_{30} mode in the $\hat{z}$ direction, in the input uniform rectangular waveguide. The first five resonant frequencies of the trapped TE_{30} mode obtained from (7) are shown in Table 3, together with results from Cascade simulation. It can be seen that (7) gives an excellent estimation of the resonant frequencies of trapped TE_{30} modes.

5. CONCLUSION

The phase of the reflection coefficient at the cut-off point of TE_{10} mode in a gentle rectangular downtaper has been verified to be +90° within a reasonably good approximation, through both the experiment and computer simulation. The +90° phase shift at the cut-off point has to be taken into account in the estimation of the resonant frequencies of spurious trapped modes in microwave resonant structures.

ACKNOWLEDGMENT

The authors would like to thank Dr. Jeffrey Neilson of Calabazas Creek Research for allowing us to use the Cascade software, based on a mode matching method, to simulate multi-mode waveguides.

REFERENCES

1. Edgcombe, C. J., *Gyrotron Oscillators — Their Principles and Practice*, Taylor and Francis, London, 1993.
2. Gold, S. H. and G. S. Nusinovich, "Review of high-power microwave source research," *Rev. Sci. Instrum.*, Vol. 68, No. 11, American Institute of Physics, Nov. 1997.
3. Nusinovich, G. S., A. N. Vlasov, and T. M. Antonsen, Jr., "Nonstationary phenomena in tapered gyro-backward-wave oscillators," *Physical Review Letters*, Vol. 87, No. 21, Dec. 19, 2001.
4. Spassovsky, I., E. S. Gouveia, S. G. Tantawi, B. P. Hogan, W. Lawson, and V. L. Granatstein, "Design and cold testing of a compact TE_{01} to TE_{20} mode converter," *IEEE Transactions on Plasma Science*, Vol. 30, No. 3, Part I, 787–793, Jun. 2002.
5. Pohl, D. W., W. Denk, and M. Lanz, "Optical stethoscopy: Image recording with resolution $\lambda/20$," *Applied Physics Letter*, Vol. 44, 651, 1984.
6. Knoll, B., A. Kramer, and R. Guckenberger, "Contrast of microwave near-field microscopy," *Applied Physics Letter*, Vol. 70, 2667, 1997.
7. Matsumaru, K., "Reflection coefficient of E-plane tapered waveguides," *IRE Transactions on Microwave Theory and Techniques*, Vol. 6, No. 2, 143–149, Apr. 1958.
8. Johnson, R. C., "Design of linear double tapers in rectangular waveguides," *IRE Transactions on Microwave Theory and Techniques*, Vol. 7, 374–378, Jul. 1959.
9. Knoll, B. and F. Keilmann, "Electromagnetic fields in the cutoff regime of tapered metallic waveguides," *Optics Communications*, Vol. 162, No. 4–6, 177–181, Apr. 15, 1999.
10. Katsenelenbaum, B. Z., L. Mercader Del Rio, M. Pereyaslavets, M. S. Ayza, and M. Thumm, "Theory of nonuniform waveguides, the cross-section method," *IEE Electromagnetic Waves*, London, UK, 1998.
11. Xu, C. and L. Zhou, "Microwave open resonators in gyrotrons," *Infrared and Millimeter Waves*, Vol. 10, 311–359, Academic Press, 1983.